Quantum chemical topology at the spin–orbit configuration interaction level: Application to astatine compounds

Cecilia Gomez Pech, Pi A.B. Haase, Dumitru-claudiu Sergentu, Anastasia Borschevsky, Julien Pilmé, Nicolas Galland, Rémi Maurice

Quantum chemical topology at the spin-orbit configuration interaction level: Application to astatine compounds

Cecilia Gomez Pech,[1,2] Pi A. B. Haase,[3] Dumitru-Claudiu Sergentu,[1,4] Anastasia Borschevsky,[3] Julien Pilmé,[5] Nicolas Galland,[2,*] and Rémi Maurice[1,†]

[1]*SUBATECH, UMR CNRS 6457, IN2P3/IMT Atlantique/Université de Nantes, 4 rue A. Kastler, 44307 Nantes Cedex 3, France*

[2]*CEISAM, UMR CNRS 6230, Université de Nantes, 2 rue de la Houssinière, 44322 Nantes Cedex 3, France*

[3]*Van Swinderen Institute for Particle Physics and Gravity, University of Groningen, Nijenborgh 4, 9747AG Groningen, The Netherlands*

[4]*Department of Chemistry, University at Buffalo, The State University of New York, Buffalo, New York 14260-3000, United States*

[5]*Sorbonne Universités, UMPC Univ. Paris 06, CNRS, Laboratoire de Chimie Théorique, cc 137, 4 place Jussieu, 75252 Paris Cedex 05, France*

(Dated: May 25, 2020)

Abstract

We report a methodology that allows the investigation of the consequences of the spin-orbit coupling by means of the QTAIM and ELF topological analyses performed on top of relativistic *and* multiconfigurational wave functions. In practice, it relies on the "state-specific" natural orbitals (expressed in a Cartesian Gaussian-type orbital basis) and their occupation numbers for the quantum state of interest, arising from a spin-orbit configuration interaction calculation. The ground states of astatine diatomic molecules (AtX with X = At–F) and triatomic anions ($IAtI^-$, $BrAtBr^-$ and $IAtBr^-$) are studied, at exact two-component relativistic coupled cluster geometries, revealing unusual topological properties as well as a significant role of the spin-orbit coupling on these. In essence, the presented methodology can also be applied to the ground and/or excited states of any compound, with controlled validity up to including elements with active 5d, 6p and/or 5f shells, and potential limitations starting with active 6d, 7p, and/or 6f shells bearing strong spin-orbit couplings.

Keywords: Topology; ELF; QTAIM; CASSCF; spin-orbit configuration interaction.

*Electronic address: nicolas.galland@univ-nantes.fr

†Electronic address: remi.maurice@subatech.in2p3.fr

I. INTRODUCTION

The description of chemical bonds in computational quantum chemistry typically requires defining (i) a quantum chemistry level of theory for computing the wave function and/or the electron density of the quantum state(s) of interest and (ii) a philosophy to map the computed information into (simple) topological models, such as the Lewis structures or the covalent-ionic paradigm of Pauling. Various approaches are available, each of them bearing advantages and drawbacks due to their intrinsic degrees of arbitrariness. However, most of them have demonstrated an indisputable utility for understanding molecular structures and even for helping chemists in the rational design of systems with desired properties.

In this work, we focus on heavy element systems which exhibit ground state bonding patterns that are greatly influenced by relativistic effects, and which are yet not fully understood by chemists. Undoubtedly, especially for the 5d, 6p and 5 f elements, the relativistic effects are usually essential to the description of chemical bonding [1]. It is well known that the 'scalar' relativistic effects, *i.e.* the ones associated with a modification of the electron kinetic and potential energies, may significantly perturb chemical bonds. In contrast, the key role of the spin-orbit coupling (SOC) is difficult to assess, not only because of severely increased computational costs, but also because of the difficulty to express it in terms of simple chemist's models. Consequently, it is too often neglected in published works [2–4]. Within a molecular orbital (MO) picture, by mixing the σ, π, *etc.* bonding and/or antibonding characters, the SOC can lead to a significant bond lengthening in heavy-element systems. For instance, the SOC lengthens the bond distance in the hypothetical At_2 diatomic molecule by $\sim$0.1 Å, this result being apparently independent of the retained quantum chemistry methodology [5–9].

Actually, astatine (At, $Z = 85$) is a good example for evidencing large SOC effects in molecules since both its free atom and its At^+ free ion display large spin-orbit splittings in their ^{2}P and ^{3}P ground 'spin-orbit-free' (SOF) states, respectively [8]. In several molecular systems, At adopts the neutral or the +I oxidation state, meaning that the molecular ground states may be significantly influenced by SOC effects, unless these are largelly quenched.

To evidence the role of the SOC on the chemical bonds, several strategies have been employed in the recent years: either (i) compute natural orbitals (spinors) in the Hilbert space and then effective bond orders (EBOs) [10] in the presence or absence of the SOC (see

[8, 9, 11–15]), or (ii) determine the electron density in the real space, its topology (QTAIM) [16], as well as that of the electron localization function (ELF) [17, 18] at relativistic DFT levels with or without the SOC (see [7, 19–28] for case studies).

Even though topological analyses on top of relativistic DFT calculations can be quite insightful, these may suffer from several theoretical or practical issues: (i) in principle, relativistic (four-component) DFT does not lead to uniqueness of the ground state density even in the case of a non-degenerate ground state [29, 30], (ii) many excited states may not be accessible (though some may be, in particular the ones that can be satisfactorily treated with the ΔSCF approach [31], *i.e.* the ones that can be properly converged via an SCF procedure), and (iii) some systems and/or quantum states may require a multiconfigurational treatment. Therefore, a new approach that addresses all these points is desirable. After presenting our proposal for doing so at the spin-orbit configuration level (SOCI), details of the implementation will be given, prior to discussing two series of compounds, namely the AtX (X = At–F) dihalogens as well as the $IAtI^-$, $BrAtBr^-$ and $IAtBr^-$ trihalide anions. Note that some of these systems exist in solution [32, 33] and have attracted a strong interest in the field of halogen-bond interactions [34, 35].

II. THEORY AND METHODS

A. Proposal and implementation

In previous work [8, 36, 37], we have shown that two-step approaches, for which the SOC is introduced *a posteriori*, are suitable for describing astatine bound systems in terms of the bond distances and also, more importantly, of the wave functions. The astatine case is key to generalize to all the heavy elements in the sense that it is the heavy element with the stronger SOC: thus, the two-step approach is meant to be valid for the bound states of systems with up to heavy elements, while the occurrence of active 6d, 7p and/or 6f shells may lead to a too strong SOC for such a treatment.

In these approaches, the first step of the calculation is SOF, meaning that the SOC operator is absent. In practice, it consists of performing a standard quantum chemistry calculation, accounting for the scalar-relativistic effects via the use of an appropriate (said 'transformed') one-electron Hamiltonian [38–45] or of a scalar-relativistic pseudopotential

[46]. Notably, we have shown on the challenging At_2 case that the wave function that is obtained with small-core energy-consistent pseudopotentials is of same quality as the one arising from all-electron calculations [8, 9], meaning that both types of calculations can be alternatively used in the present context for bonding analyses.

The multiconfigurational calculations typically start with a state-average complete active space self-consistent field (SA-CASSCF) step, eventually supplemented by a more correlated post-CASSCF treatment [47–53]. The second step consists of diagonalizing the $\mathbf{H}_{\text{tot}} = \mathbf{E}_{\text{el}} + \mathbf{H}_{\text{SOC}}$ matrix within the basis of the spin (*i.e.* M_S) components of the previously obtained SOF states. By mixing the components of the SOF states, the SOC operator leads to sizeable changes in the wave function [8, 9, 12, 54], which can be monitored in terms of the occupation numbers (ONs) of the natural orbitals (NOs) [55, 56].

The role of the SOC on the NOs and their corresponding ONs for a given quantum state of interest is quite clear [9]: (i) if symmetry prevents rotations between the active orbitals, the NOs are maintained, meaning that only the ONs are susceptible to be updated and (ii) if symmetry allows for rotations between the active orbitals, the NOs need to be revised (and so do the ONs). In any case, we encounter a situation that is similar to any configuration interaction (CI) case, meaning that the role of the SOC may be accounted for in exactly the same way as the one of electron correlation can be.

The original ELF formulation of Becke and Edgecombe [17] was designed for single-reference wavefunctions. Later, the ELF kernel $\chi(\mathbf{r})$ was extended in a functional form by Savin and coworkers [57], who also proposed an interpretation of the ELF in terms of the local kinetic energy excess due to the Pauli repulsion:

$$\text{ELF}(\mathbf{r}) = \frac{1}{1+\chi(\mathbf{r})^2} \tag{1}$$

with:

$$\chi(\mathbf{r}) = \frac{T_s(\mathbf{r}) - \frac{1}{4}\frac{|\nabla\rho(\mathbf{r})|^2}{\rho(\mathbf{r})}}{2\,C_F\rho(\mathbf{r})^{5/3}} \tag{2}$$

In this latter formulation, $T_s(\mathbf{r})$ is the positive definite local kinetic energy of non-interacting electrons, $\rho(\mathbf{r})$ is the total electron density and C_F is a constant $[\frac{3}{10}(3\pi^2)^{\frac{2}{3}}]$. This formulation was also restricted to single-determinant wave functions (*e.g.* a Kohn-Sham DFT one).

Fifteen years later, the role of electron correlation on the ELF was introduced in a fashion

that was based on the Laplacian of the conditional same-spin pair function $\pi^{\sigma\sigma}$ [58]:

$$\chi(\mathbf{r}) = \frac{\nabla_s^2 \pi^{\sigma\sigma}(\mathbf{r}, \mathbf{r}+\mathbf{s})|_{\mathbf{s}\to\mathbf{0}}}{C_F[2\rho^\sigma(\mathbf{r})]^{8/3}} \tag{3}$$

Although the pair function can be easily written in terms of molecular orbitals, eq. (3) has only been used at the CISD level for some light atoms or small diatomic molecules, the computational effort being several orders of magnitude larger than for a monodeterminantal wave function. Even for triatomic molecules of the first-row elements, its application remains rather difficult. Hence, Feixas *et al.* [59] have proposed to compute the ELF kernel by using a Hartree-Fock like approximation of the pair function defined in terms of natural spin orbitals. Even if the correlation effects are rather large (as it is the case for H_2O_2), this orbital scheme yield values in very good agreement at CASSCF level of theory.

Actually, a two-fold approximation requiring only the updated NOs and their corresponding ONs can be used [59], quantities which, as mentioned above, can be readily computed *after* the introduction of the SOC operator. First, we use a single-determinant approximation for computing the two-particle density matrix and thus the ELF [60, 61]. Second, Buijse and Baerends' first approximation [62, 63] is considered for computing the (basin) populations. This two-fold approximation which has been validated for CASSCF wavefunctions, *i.e.* for multiconfigurational wave functions expanded in terms of Slater determinants or of configuration state functions (CSFs). Since the SOCI wave functions are nothing but a further expansion of the CASSCF ones in the basis of the M_S components of the CASSCF solutions, one could thus readily reexpand them in terms of Slater determinants or of CSFs, meaning that these approximations must also be valid at the SOCI level. Therefore, we apply these without further justification. Also, this makes clear that a non-relativistic expression for the ELF also applies in the SOCI framework.

The delocalization index [64, 65], noted $\delta(\Omega_A, \Omega_B)$, measures the electron pair sharing between two atomic basins Ω_A and Ω_B. Although it can be properly defined from the covariance matrix (twice the covariance matrix element), its practical evaluation remains difficult in the framework of correlated wave functions. Interestingly, Wang and Werstiuk [66] have proposed an approximated expression to compute $\delta(\Omega_A, \Omega_B)$ from (molecular) NOs:

$$\delta(\Omega_A, \Omega_B) = 2 \sum_i \sum_j n_i^{1/2} n_j^{1/2} \langle\varphi_i|\varphi_j\rangle_{\Omega_A} \langle\varphi_i|\varphi_j\rangle_{\Omega_B} \tag{4}$$

where n_i and n_j are the occupation numbers of the φ_i and φ_j NOs, respectively. Naturally, this expression simplifies with orthogonal MOs (only the $i = j$ cases apply), as in the present work, the total local density being:

$$\rho(\mathbf{r}) = \sum_i n_i \varphi_i^*(\mathbf{r}) \varphi_i(\mathbf{r}) \tag{5}$$

The effect of Coulomb correlation is now included and $\delta(\Omega_A, \Omega_B)$ remains invariant with respect to any unitary transformation of the orbitals. Thus, for defining all the targeted topological descriptors at the SOCI level, we basically need to compute the NOs and their corresponding ONs.

Actually, these quantitites can readily be obtained from a SOCI calculation according to the methodology described in [9] (see also [12] and [67]). At this stage, only an interface with a topological analysis program is thus needed. In this work, we have selected the TopMoD program [68], that is capable of performing both QTAIM and ELF types of topological analyses. Due to restrictions in TopMoD, the NOs retrieved from the SOCI calculations must be expanded within an uncontracted Cartesian Gaussian-type basis. This has two consequences: (i) the initial quantum chemistry calculations must be performed with a Cartesian Gaussian-type basis and (ii) one must switch from the contracted set to the primitive one, which may require attention in terms of the ordering and normalization.

In practice, we have used the MOLPRO program [69] for the SOCI calculations, since it is capable of handling Cartesian Gaussian-type basis functions in conjunction with pseudopotentials that include SOC operators. Furthermore, since Cartesian Gaussian-type basis functions may be expressed as [70, 71]:

$$\phi_A(\boldsymbol{r}) = N(x - A_x)^l (y - A_y)^m (z - A_z)^n \, \mathrm{e}^{-\alpha(\boldsymbol{r} - \boldsymbol{A})^2} \tag{6}$$

a normalization factor applies between the contracted set and the primitive one [70, 71]:

$$N = \left(\frac{2\alpha}{\pi}\right)^{3/4} \left[\frac{(8\alpha)^{l+m+n} l!m!n!}{(2l)!(2m)!(2n!)}\right]^{1/2} \tag{7}$$

All the information required by TopMoD is extracted from the MOLPRO output using a Python interface that handles both the ordering and normalization issues, and delivers the information into a WFN-type file. The program code is freely available upon request.

B. Computational details

1. *Exact two-component coupled cluster calculations*

The determination of *reference* molecular geometries for heavy-element systems requires an appropriate and simultaneous treatment of relativistic effects and of electron correlation. If one electronic configuration can be used as a reliable zeroth-order wave function, the single-reference coupled cluster method including single, double and perturbative triple excitations [CCSD(T)] [72] constitutes a "gold" standard for doing so. In the context of astatine chemistry, this was confirmed for the non-trivial AtO^+ ion for which a comparison between single-reference and multireference relativistic coupled cluster calculations has been previously reported [73]. Also, the relativistic Hamiltonian may be either a four-component one or a two-component one [38–43, 45], with typically an exceptionally good agreement between the results obtained with four-component and exact two-component (X2C) [44] formalisms.

In previous work [9], we have determined molecular geometries for the AtX (X = At–F) systems at the X2C level [44, 45] using the DIRAC15 code [74]: 2.967 Å for At_2, 2.816 Å for AtI, 2.614 Å for AtBr, 2.471 Å for AtCl and 2.045 Å for AtF. These geometries will be retained for the further single-point calculations (*vide infra*). Note that in the At_2 case, the X2C CCSD(T) geometry is well reproduced at the SOCI level (*e.g.* 2.957 Å in [8] with the "contracted" SOCI scheme). Also, we have shown that Dyall's relativistic basis sets of quadruple-zeta augmented with one set of diffuse functions per angular-momentum block (AVQZ) [75, 76] lead to practically the same molecular geometries than the non-augmented versions, *i.e.* VQZ, for the dihalogen molecules (AtX with X = At–F), which shows that this property is reasonably converged with the VQZ basis set. Therefore, in this work, we have used the DIRAC15 code to numerically determine the *reference* geometries for the $IAtI^-$, $BrAtBr^-$ and $IAtBr^-$ triahalide anions at the X2C [45] CCSD(T) [72] level, with Dyall's AVQZ ($IAtI^-$ and $BrAtBr^-$) or VQZ ($IAtBr^-$) basis sets [75, 76]. All the orbitals within the −20 to 30 a.u. energy range have been correlated, as previously done for the dihalogen molecules [9]. Note that the atomic nuclei have been described beyond the point charge approximation via a Gaussian nuclear model [77]. Non-relativistic and scalar-relativistic CCSD(T) calculations have also been performed in order to highlight the role of the scalar-

relativistic and spin-dependent effects on the molecular geometries.

2. Spin-orbit configuration interaction calculations

All the SOCI calculations have been performed at the X2C CCSD(T) geometries with the MOLPRO program. The SA-CASSCF calculations relied on active spaces that comprise the valence np shells of the halogens, in particular consisting of 10 electrons correlated within 6 orbitals (dihalogen molecules) or 16 electrons within 9 orbitals (trihalide anions). For all the computed SOF states, the "electronic" energies have been computed using the strongly-contracted n-electron valence state second-order perturbation theory (NEVPT2) [51–53]. The latter were used to dress the diagonal of the $\mathbf{H}_{\rm tot} = \mathbf{E}_{\rm el} + \mathbf{H}_{\rm SOC}$ matrix.

The number of SOF states retained for the SA-CASSCF calculations has been selected in order to reproduce more than 99 % of the SOC wave function that is obtained with the full space of SOF states. For instance, for any of the AtX (X = I–F) systems, a computation with 1 spin-singlet state and the three M_S components of 4 spin-triplet roots recovers more than 99 % of the wave function that is obtained with 21 spin-singlet roots and the spin components of 15 spin-triplet roots for the considered active space [9]. The ground state of the At_2 system, by symmetry, only requires the components of 2 spin-triplet roots. However, for comparison purposes, it is wise to have the same spaces for the entire series. Therefore, the present At_2 calculations were also based on 1 spin-singlet state and the components of 4 spin-triplet roots. Test calculations have shown that the ground states of the three studied trihalide anions, namely $IAtI^-$, $BrAtBr^-$ and $IAtBr^-$, can also be well described using 1 spin-singlet state and 4 spin-triplet roots. Therefore, this space was eventually selected for describing all the reported systems.

Scalar-relativistic plus SOC pseudopotentials [78, 79] were used for describing the heaviest atoms, namely At, I and Br. For avoiding linear dependencies in the calculations with the Cartesian Gaussian-type bases, we have considered basis sets of triple-zeta quality, namely aug-cc-pVTZ-PP [78, 79] for the heaviest atoms and aug-cc-pVTZ [80, 81] for the remaining ones.

3. Determination of the "state-specific" natural orbitals and topological analyses

The outcome of the SOCI calculations are multiconfigurational wave functions expressed in terms of the M_S components of the SOF states. Thus, in the MOLPRO calculations, the one-electron density matrices were stored for all the SOF states (corresponding to 1 spin-singlet and 4 spin-triplet roots). Then, the one-electron density matrix of the ground SOC states were generated by applying the appropriate weighted sum of the density matrices of the SOF states, exactly in the same way as in previous work dedicated to EBOs [9]. By diagonalizing this weighted sum of density matrices, the "state-specific" NOs of the ground SOC states are obtained [54], together with their ONs. Finally, WFN files containing these NOs and the corresponding ONs are generated using the newly developed Python interface (*vide supra*).

The WFN files serve as input files for the QTAIM and ELF topological analyses that are performed with the TopMoD09 program. Note that all the calculations have been performed in the C_1 symmetry point group. 12x12x18 bohr grids have been considered for the dihalogen molecules, and 12x12x24 bohr grids for the trihalide anions, all built with a step of 0.05 bohr.

In the QTAIM topological analyses, only atomic basins are expected, as well as one bond critical point (BCP, denoted as 'CP' in the remainder of the text) for each independent pair of adjacent atoms. We recall here that an atomic basin is a region of the 3D space for which the maximum of the density (*i.e.* the density value at the atomic position, the cusp) can be seen as an attractor of the gradient field. A CP is the intersection between the bond segment and the zero-flux surface that separates the two atomic basins. In the ELF topological analyses, more basins may be obtained, typically one core –C(X)– basin and one valence monosynaptic –V(X)– basin for each X atom plus possibly one valence disynaptic –V(X,Y)– basin for each independent pair of X and Y adjacent atoms. Note that a valence monosynaptic basin is connected only to one core basin (one can thus think of a "lone pair"), while a valence disynaptic one connects to two distinct core basins, *i.e.* they have a boundary with the cores of two distinct atoms. In other words, one may refer to these basins as "bonding basins". Integration of the electron density over a basin volume provides its population.

III. RESULTS AND DISCUSSION

A. First set: the AtX (X = At–F) series

The AtX (X = At–F) series constitutes our first set of systems. The series is interesting for two main reasons, (i) computational data related to chemical bonding is available, with reported DFT topologies [7, 21] as well as SOCI EBOs [8, 9], and (ii) some of the systems (AtI, AtBr and AtCl) are of experimental relevance [32, 33].

We start our discussion with the QTAIM bonding descriptors (see Table I). The At atomic charges, q(At), have been determined by integrating the electron density over the At atomic basin, giving rise to an electron number to be substracted from the electron count of neutral At (here 25 electrons due to the use of the 'small-core' ECP60MDF pseudopotential [78]). Three descriptors are determined at the CP, the value of the electron density ($\rho_{\rm CP}$), its Laplacian ($\nabla^2\rho_{\rm CP}$), and the ratio between the absolute potential energy density and the positive-definite kinetic energy density ($|V_{\rm CP}|/G_{\rm CP}$). Finally, the delocalization index (δ) is determined from the covariance matrix.

In the series, the At charge is regularly increasing, up to 0.58 in AtF, reflecting a quite ionic character in this system, as expected. The $\rho_{\rm CP}$ values are smaller than 0.1 in the AtX (X = At–Cl) cases and the Laplacians of the density are positive (excess of kinetic energy density at the CP with respect to the local virial theorem), suggesting *closed-shell* interactions according to the standard QTAIM classification [16]. However, the $|V_{\rm CP}|/G_{\rm CP}$ ratios larger than 1 suggest some covalency since the potential energy density tends to stabilize electrons at the CP. The delocalization index, if taken as a measure of the bond order [82], suggests that AtI is the most covalent system of the series (δ = 0.90). The AtF system displays unique features in the series, *e.g.*, a quite large Laplacian value in line with an ionic bond, but also a $|V_{\rm CP}|/G_{\rm CP}$ ratio larger than 1, suggesting that this bond is not fully ionic but that it rather contains some covalent character as well. The calculated delocalization index, 0.72, is furthermore much larger than those reported for model ionic molecules ($\approx$ 0.2 for NaCl and LiH [82]).

The ELF topological descriptors include populations, with the atomic basin populations referred to as C+V(X) in Table I, and the bonding basin ones referred to as V(At,X). The variances of the V(At,X) populations (σ^2) as well as the relative population fluctuations

TABLE I: Selected QTAIM and ELF topological descriptors (in a.u.) for the AtX series (X = At–F), computed at X2C CCSD(T) geometries [9]. The spin-orbit coupling contribution to each descriptor is given in parenthesis.

X	QTAIM					ELF				
	q(At)	ρ_{CP}	$\nabla^2\rho_{CP}$	$\lvert V_{CP}\rvert/G_{CP}$	δ	C+V(At)	C+V(X)	V(At,X)	σ^2	λ
At	0.01	0.050	0.032	1.58	0.78	24.73	24.74	0.51	0.43	0.84
	(0.00)	(0.000)	(0.006)	(−0.05)	(−0.14)	(0.03)	(0.07)	(−0.09)	(−0.07)	(0.01)
I	0.10	0.061	0.027	1.72	0.90	24.61	24.72	0.66	0.54	0.82
	(0.00)	(0.000)	(0.005)	(−0.04)	(−0.10)	(0.03)	(0.06)	(−0.07)	(−0.05)	(0.01)
Br	0.23	0.072	0.053	1.61	0.88	24.55	24.89	0.54	0.46	0.85
	(0.00)	(0.000)	(0.006)	(−0.03)	(−0.10)	(0.05)	(0.08)	(−0.13)	(−0.08)	(0.05)
Cl	0.34	0.081	0.084	1.56	0.84	24.51	17.06	0.42	0.36	0.86
	(0.00)	(0.000)	(0.006)	(−0.02)	(−0.14)	(0.06)	(0.05)	(−0.10)	(−0.08)	(0.01)
F	0.58	0.109	0.381	1.25	0.72	24.44	9.54	NA[a]	NA	NA
	(0.01)	(0.001)	(−0.001)	(0.01)	(−0.10)	(0.01)	(−0.01)	NA	NA	NA

[a]NA denotes not applicable.

$[\lambda = \sigma^2/\mathrm{V(At,X)}]$ are also given. Three types of topologies have been obtained (see Figure 1): symmetric with a valence disynaptic basin (At_2), asymmetric with such a basin (AtX with X = I–Cl), and asymmetric with no disynaptic basin (AtF).

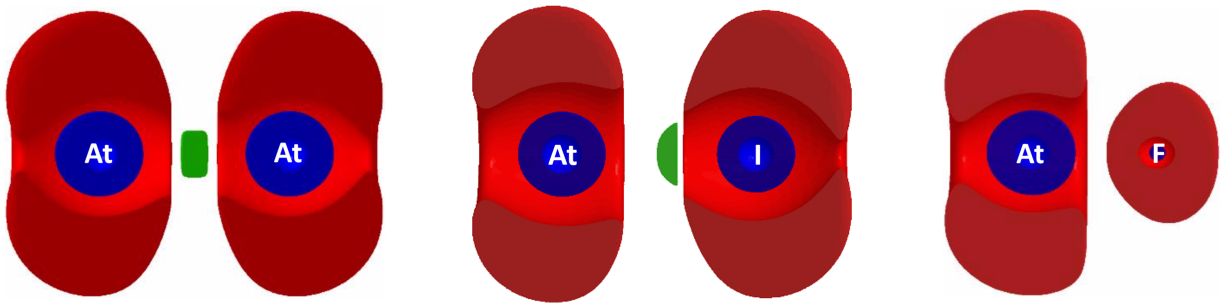

FIG. 1: Representative isosurfaces of the three typical ELF topologies obtained for the AtX series (X = At–F): At_2 (left, isosurface = 0.470), AtI (middle, isosurface = 0.557) and AtF (right, isosurface = 0.450), computed at X2C CCSD(T) geometries [9]. Color code: blue stands for core and red for valence monosynaptic basins, green for valence disynaptic basins.

We recall here that a population of *ca.* 2 electrons for a valence disynaptic basin is characteristic of a single (covalent) bond. In the X = At–Cl cases, about half an electron is found in the valence disynaptic basins. V(At,I) has actually the maximal population within the series, which is in line with a maximum of the covalent character for X = I, in accord with the previous remark on the delocalization index. For all the X = At–Cl systems, the relative fluctuations λ are about 85 %, which may be indicative of a significant charge-shift (CS)

character in these bonds [83–85]. In the At_2 case, symmetry imposes both the At^- $At^+ \leftrightarrow$ At—At and At—At $\leftrightarrow$ At^+ At^- iono-covalent resonances to be equivalent. Consequently, these two resonances contribute to the CS character of the bond (*i.e.* to the At^- $At^+ \leftrightarrow$ At^+ At^- effective resonance). In the X $\neq$ At cases, the two iono-covalent resonances are not symmetry equivalent, meaning that the sum of the two may contribute both to a CS character and to a simpler iono-covalent character. Therefore, we conclude that signatures of CS bonding have been obtained in the X = At–Cl cases, while it is clear that the ELF topology of the AtF system also points to an ionic bond since the C+V(At) and C+V(X) populations largely differ from the ones that would be expected for the neutral situation, *i.e.* 25 and 9, respectively. Note that signatures are not definitive proofs for CS bonding; a valence bond (VB) study may be desired to fully elucidate the bonding in the X = At–Cl cases, which is out of the scope of the present work.

In Table I, the contributions of the SOC to topological descriptors are given in parentheses. Concerning the QTAIM descriptors, though q(At), ρ_{CP} and $\nabla^2\rho_{CP}$ seem almost practically unaffected by the SOC, noticeable effects are seen for $|V_{CP}|/G_{CP}$ and δ, two important bonding descriptors. Typically, it diminishes these two quantities, which may be interpreted as a weakening of the covalent character. Such weakening is also seen from the topology of the ELF, with significant drops of the populations of the valence disynaptic V(At,X) basins. Moreover, it is also in line with the conclusions of our previous study on EBOs [9]. The relative fluctuations λ are slightly increased by the SOC, which may indicate a slight reinforcement of the CS character in these bonds. This may be explained in an MO picture: here, from the ground $\sigma^2\pi^4\pi^{*4}$ electronic configuration, the SOC essentially triggers the $\pi \rightarrow \sigma^*$ (all the series) and $\pi^* \rightarrow \sigma^*$ (only if X $\neq$ At) single excitations [9], meaning that it promotes the $\sigma^2\sigma^{*1}$ electronic subconfiguration in the SOC ground state wave function, thus enhancing charge fluctuation [86].

A last point worth being commented concerns the comparison of the obtained topological descriptors to the previous DFT ones [21]. Although the SOC contributions to the descriptors should not be directly compared (here, single-point calculations at the X2C geometries *versus* differences calculated between optimized scalar-relativistic and quasi-relativistic geometries in [21]), it may be interesting to compare trends. Overall, similar trends are obtained, with a notable exception for the populations of the V(At,X) basins: at the SOCI level, these populations regularly decrease from X = I to X = Cl, while an increase of this

population was obtained for X = Cl at the DFT level. This difference may result from (i) multiconfigurational characters of the ground state wave functions, better described in the present work and/or (ii) differences in the treatment of "dynamic" correlation. Therefore, our new multiconfigurational methodology may be crucial for revealing fine trends, especially when the multiconfigurational characters of the quantum states vary within a series.

B. Second set: the $IAtI^-$, $BrAtBr^-$ and $IAtBr^-$ trihalide anions

For the second set, we focus only on the $IAtI^-$, $BrAtBr^-$ and $IAtBr^-$ trihalide anions. These have been evidenced in solution [33] and are valence isoelectronic with the triiodide I_3^- system [87]. Their electronic structures potentially involve several important (Lewis) structures in a VB framework: X_1—At$\cdots X_2^-$ (a "partly-ionic" structure involving one covalent bond plus one halogen-bond interaction), X_1^- At^+ X_2^- (the "fully-ionic" structure) and $X_1^-\cdots$At—X_2 (the other "partly-ionic" structure), as in I_3^- [88], and also perhaps the $X_1^\bullet$ At^- $X_2^\bullet$ diradical structure [89], which has lead for instance in F_3^- to a significant CS bonding character [88]. Therefore, because of symmetry, one may think of a given bond as a kind of mixing between a covalent bond, an ionic bond and a halogen bond in $IAtI^-$ and $BrAtBr^-$, meaning that the QTAIM and ELF topologies must reveal significant differences with the bonds in the studied trihalide anions *versus* the ones in the corresponding dihalogen molecules (namely AtI and AtBr). However, since the $IAtBr^-$ trihalide anion does not possess an inversion center, it is possible in this system to end up with one dominant structure (I—At$\cdots Br^-$ or more probably $I^-\cdots$At—Br), *i.e.* with a halogen-bonded adduct. As for the diatomics, we would like to recall that if a given wave function is multiconfigurational within a VB framework, this does not mean that it is also the case within an MO one; here, the single-reference CCSD(T) approach is well suited.

1. *Exact two-component geometries*

The $IAtI^-$, $BrAtBr^-$ and $IAtBr^-$ trihalide anions are linear systems (see Figure 2), the most polarizable At atom being placed in between the two other ones, as expected [90]. Previous scalar-relativistic [91] and quasi-relativistic [33] DFT geometries have been reported in Table II for comparison purposes with the new reference non-relativistic, scalar-relativistic

TABLE II: Non-relativistic, scalar-relativistic and X2C bond distances (Å) for the $IAtI^-$, $BrAtBr^-$ and $IAtBr^-$ trihalide anions obtained with coupled-cluster calculations including single, double and perturbative triple excitations, CCSD(T). DFT results based on the B3LYP [92, 93] exchange-correlation functional and small-core energy-consistent pseudopotentials [78, 79] are also given.

System	Bond(s)	Non-relativistic	Scalar-relativistic		Quasi-relativistic	X2C
		CCSD(T)	DFT [91]	CCSD(T)	DFT [33]	CCSD(T)
$IAtI^-$	I–At (×2)	3.038	3.08	2.986	3.15	3.033
$BrAtBr^-$	Br–At (×2)	2.810	2.86	2.777	2.91	2.823
$IAtBr^-$	I–At	3.027	3.07	2.974	3.14	3.029
	At–Br	2.819	2.87	2.789	2.92	2.823

and X2C geometries.

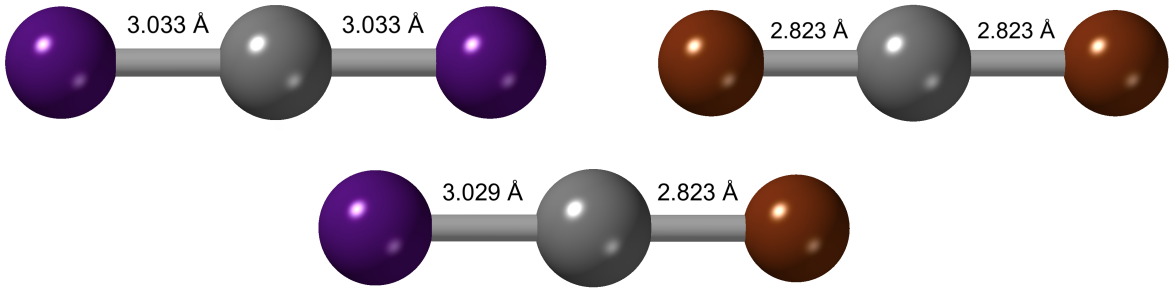

FIG. 2: Ball and stick representations of the X2C CCSD(T) geometries of the $IAtI^-$ (top left), $BrAtBr^-$ (top right) and $IAtBr^-$ (bottom) triahalide anions. Color code: grey stands for At, purple for I and brown for Br.

As expected, the X2C bond distances are significantly larger than the ones of the dihalogen molecules (2.816 Å for AtI and 2.614 Å for AtBr, respectively [9]), in line with a significant contribution of halogen bonding to the bonds in the $IAtI^-$ and $BrAtBr^-$ symmetric systems. $IAtBr^-$ displays interesting bond distances practically identical to those calculated in the parent $IAtI^-$ and $BrAtBr^-$ systems, meaning that none of the I—At and At—Br bonds in $IAtBr^-$ can be a "pure" halogen bond. In other words, similarities can be expected between these bonds and the ones of the parent $IAtI^-$ and $BrAtBr^-$ systems.

As can be seen in Table II, the summed relativistic effects leave in appearance the bond distances almost intact (the scalar-relativistic bond contractions almost perfectly cancel the SOC bond expansions of about 0.05 Å). The situation is quite distinct from that of the parent dihalogen molecules. Indeed, in the dihalogen molecules, we have previously obtained scalar-relativistic bond contractions of about 0.02 Å (*i.e.* half that obtained here) and SOC

TABLE III: Selected QTAIM topological descriptors (in a.u.) for the studied $X_1AtX_2^-$ trihalide anions, computed at X2C CCSD(T) geometries. The spin-orbit coupling contribution to each descriptor is given in parenthesis.

X_1	X_2	Atomic charges			X_1—At bond				At—X_2 bond			
		$q(X_1)$	q(At)	$q(X_2)$	ρ_{CP}	$\nabla^2\rho_{CP}$	$\lvert V_{CP}\rvert/G_{CP}$	δ	ρ_{CP}	$\nabla^2\rho_{CP}$	$\lvert V_{CP}\rvert/G_{CP}$	δ
I	I	−0.54	0.15	−0.54	0.042	0.043	1.41	0.64	0.042	0.043	1.41	0.64
		(0.00)	(0.00)	(0.00)	(0.000)	(0.001)	(0.00)	(−0.06)	(0.000)	(0.001)	(0.00)	(−0.06)
Br	Br	−0.62	0.31	−0.62	0.049	0.065	1.37	0.62	0.049	0.065	1.37	0.62
		(0.00)	(0.00)	(0.00)	(0.000)	(0.001)	(0.00)	(−0.06)	(0.000)	(0.001)	(0.00)	(−0.06)
I	Br	−0.57	0.23	−0.60	0.042	0.044	1.40	0.64	0.049	0.063	1.38	0.62
		(0.00)	(0.00)	(0.00)	(0.000)	(0.001)	(0.00)	(−0.01)	(0.000)	(0.001)	(0.00)	(0.00)

bond expansions of about 0.06–0.07 Å (*i.e.* slightly larger than here), overall resulting in bond expansions of about 0.04–0.05 Å (see [9] and references therein for a more detailed discussion regarding the respective roles of the scalar-relativistic effects and of the SOC).

A last point on the bond distances concerns the comparison of the new CCSD(T) results with the previous DFT ones [33, 91]. While the contributions of the SOC to the bond distances are of the same order of magnitude (about 0.05–0.07 Å at the DFT level), the X2C CCSD(T) geometries are about 0.1 Å shorter than the quasi-relativistic DFT ones. We continue by discussing only the topologies obtained at the X2C CCSD(T) geometries.

2. QTAIM and ELF topologies

Selected QTAIM descriptors are reported in Table III. First, the reported atomic charges highlight again that At is essentially in its zero oxidation state [33]. Naturally, the negative charge is equally distributed among the I and Br centers in the symmetric $IAtI^-$ and $BrAtBr^-$ systems. Interestingly, it is also the case in the $IAtBr^-$ system, meaning that the latter effectively behaves as if it would possess an inversion center. This is another argument in favor of a balanced resonance between covalent, ionic and halogen bondings for the I—At and At—Br bonds in this system. Also, all the other QTAIM descriptors (the ρ_{CP}'s, $|V_{CP}|/G_{CP}$'s and δ's) for the I—At and At—Br bonds are pretty similar to those for the parent symmetric anions, definitively ruling out the possibility of a dominant VB structure such as $X_1^- \cdots$ At—X_2 for the exotic $IAtBr^-$ system.

Two types of ELF topologies have been obtained (see Figure 3): symmetric ($IAtI^-$ and $BrAtBr^-$) or asymmetric ($IAtBr^-$) with two tiny valence disynaptic basins. The corre-

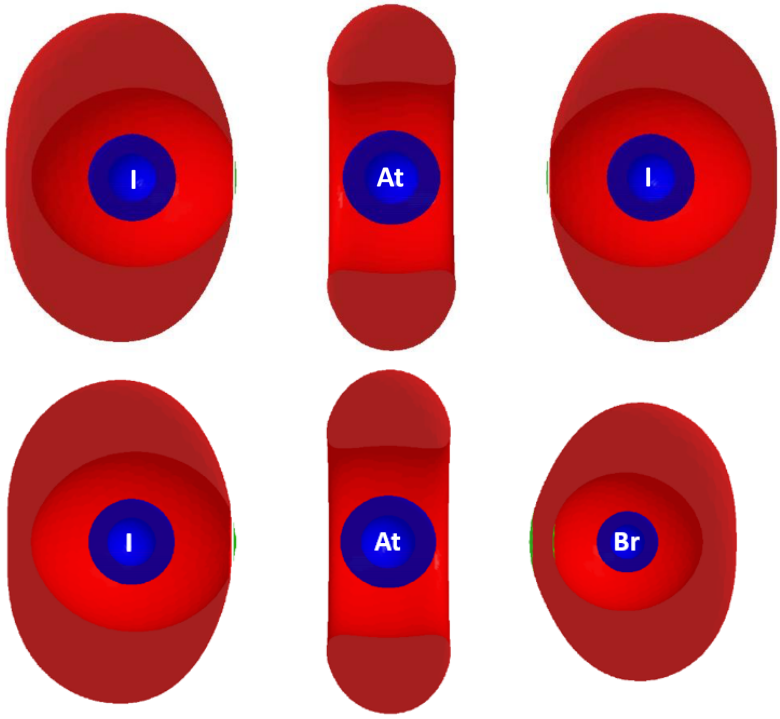

FIG. 3: Representative isosurfaces of the two typical ELF topologies obtained for the studied trihalide anions: $IAtI^-$(top, isosurface = 0.671) and $IAtBr^-$ (down, isosurface = 0.681), computed at X2C CCSD(T) geometries (see Table II). Color code: blue stands for core and red for valence monosynaptic basins, green for valence disynaptic basins.

TABLE IV: Selected ELF topological descriptors (in a.u.) for the studied $X_1AtX_2^-$ trihalide anions, computed at X2C CCSD(T) geometries. The spin-orbit coupling contribution to each descriptor is given in parenthesis.

X_1	X_2	Monosynaptic basins			X_1—At bond			At—X_2 bond		
		C+V(X_1)	C+V(At)	C+V(X_2)	V(X_1,At)	σ^2	λ	V(At,X_2)	σ^2	λ
I	I	25.41	24.66	25.41	0.23	0.21	0.91	0.23	0.21	0.91
		(0.09)	(0.03)	(0.09)	(−0.11)	(−0.10)	(0.00)	(−0.11)	(−0.10)	(0.00)
Br	Br	25.41	24.54	25.41	0.31	0.28	0.90	0.31	0.28	0.90
		(0.09)	(0.02)	(0.09)	(−0.10)	(−0.08)	(0.02)	(−0.10)	(−0.08)	(0.02)
I	Br	25.45	24.59	25.42	0.23	0.22	0.96	0.27	0.24	0.89
		(0.14)	(0.03)	(0.08)	(−0.16)	(−0.12)	(0.08)	(−0.10)	(−0.09)	(0.00)

sponding topological descriptors are reported in Table IV. As with the QTAIM analysis, the similarity between the descriptors for the $IAtBr^-$ system with the ones of the parent $IAtI^-$ and $BrAtBr^-$ systems is striking, pointing to similar bond natures in the three studied trihalide anions. The tiny valence disynaptic basins are characterized by small electron populations (at most ∼0.3), affected by very large relative fluctuations (90% or more). Recalling

TABLE V: Rescaled QTAIM atomic charges (q's) and derived VB weights (ω's, see text).

X_1	X_2	q'(X_1)	q'(At)	q'(X_2)	ω_1	ω_2	ω_3
I	I	−0.58	0.16	−0.58	0.42	0.16	0.42
Br	Br	−0.67	0.33	−0.67	0.33	0.33	0.33
I	Br	−0.61	0.24	−0.64	0.40	0.24	0.37

that we essentially expect three VB structures to play a significant role in the wave function (X_1—At$\cdots X_2^-$, X_1^- At^+ X_2^- and $X_1^-\cdots$ At—X_2), the disclosed large fluctuations may be the signature for a kind of CS bonding, associated with the effective resonance between the two "partly-ionic" VB structures. VB calculations would be desired to fully reveal it, as done in the case of the trifluoride anion F_3^- [88].

To give a first flavor of the potential weights of the more important VB structures, we propose to use the QTAIM charges, which is similar in this case to using the atomic populations, as done by Silvi and others [94, 95]. Since we have only three atomic charges, we can access to three different weights. Therefore, we consider the three following structures, with their associated weights given in parenthesis: X_1—At$\cdots X_2^-$ (ω_1), X_1^- At^+ X_2^- (ω_2) and $X_1^-\cdots$ At—X_2 (ω_3), leading in the general (*i.e.* the asymmetric) case to the following system of equations:

$$\begin{cases} q(X_1) = -\omega_2 - \omega_3 \\ q(\mathrm{At}) = \omega_2 \\ q(X_2) = -\omega_1 - \omega_2 \end{cases} \tag{8}$$

Naturally, if $q(X_1) = q(X_2)$ (the symmetric case), the system of equations simplifies. As can be seen in Table III, the (numerical) atomic charges do not perfectly sum to −1, which would translate into weights that do not sum to 1. Consequently, we have "normalized" the charges to −1 by multiplying them by a common factor (1/0.93 for $IAtI^-$ and $BrAtBr^-$, and 1/0.94 for $IAtBr^-$). The resulting charges and weights are given in Table V. Again, $IAtBr^-$ behaves as an intermediate between $IAtI^-$ and $BrAtBr^-$. The weights of the "fully-ionic" structures, X_1^- At^+ X_2^-, are in line with the trend observed for the diatomics (AtI is more covalent than AtBr) and also the electronegativity difference between the outer atoms (I or Br) and At. Finally, the small difference between ω_1 and ω_3 in $IAtBr^-$ is just another way to highlight that this system effectively behaves as a symmetric trihalide anion.

3. Discussion: bonding in the trihalide anions versus bonding in the dihalogen molecules

So far, we have compared the respective topologies of the studied trihalide anions, revealing similarities between the three compounds. To complete the discussion, these topologies must also be compared with the ones obtained for the dihalogen molecules. The atomic charges on the At centers are small and similar in AtI and AtBr and in the trihalide anions (zero oxidation state). Of course, due to the anionic character of the trihalides, the charges on the other centers are different.

The QTAIM $|V_{\rm CP}|/G_{\rm CP}$ descriptor naturally reveals a less strong covalent character in the trihalide anions than in the corresponding dihalogen molecules (see Tables I and III). It is confirmed by the smaller values of the two-center delocalization indices, the δ's, calculated for the trihalides. This also translates into much smaller populations for the ELF valence disynaptic basins (these are reduced by half from the dihalogen molecules to the trihalide anions, see Tables I and IV). Nevertheless, a finer trend reveals that the populations of the V(At,Br) basins are larger than the V(At,I) ones in the triahalide anions, unlike for the dihalogen molecules, though this may not be very chemically significant.

Benefiting from the main advantage of the proposed methodology, we can readily determine the contribution of SOC to the topological descriptors. As shown in Tables I, III and IV, the QTAIM descriptors are much less affected by the SOC in the trihalide anions, while the role of SOC on the ELF descriptors is of the same order of magnitude in the trihalide anions and in the parent dihalogen molecules, demonstrating once more that the bonding in heavy-element compounds must be analyzed after inclusion of the SOC [7–9, 15, 21, 25, 96, 97]. Actually, the hybrid characters of the bonds in the trihalide anions (covalent/ionic/halogen), which translate into larger bond distances as compared to the parent diatomic molecules, are presumably responsible for this observed trend on the QTAIM descriptors.

IV. CONCLUDING REMARKS

Following the work of Feixas *et al.* [59], we have applied for the first time the NO formulation of the ELF to correlated *and* relativistic wave functions, determined after the introduction of the SOC. In principle, this approach is valid as soon as the SOCI wave

function of the quantum state of interest is accurate enough, presumably for the ground and excited states of all the compounds that include elements with $Z \leq 103$ (above, *i.e.* for the superheavies, accounting for the SOC *a posteriori* may not be good enough). Furthermore, it is complementary to the previously developed quasi-relativistic DFT implementation [7, 21], in the sense that it does not suffer from the same issues (single-determinant approach, excited states, *etc.*).

Two main practical limitations of the present methodology, (i) the computational cost may become prohibitive if a too large active space is required at the SA-CASSCF step and (ii) state-averaging artifacts may become too important if the spin components of a too large number of SOF states are required for the SOCI step. Nevertheless, these two issues are not that often critical in everyday applications and we expect this methodology to be interesting for determining the QTAIM and ELF topologies of many main-group, transition-metal, lanthanide and/or actinide chemical systems. Naturally, the application of bonding analysis tools to At-containing systems is particularly relevant since chemical intuition is terribly lacking on this extremely rare radioelement of potential interest for nuclear medicine applications [98].

After the definition of EBOs at the SOCI level [8, 9, 12], we have now introduced the quantum chemical topology at this exact same level, allowing the definition of complementary bonding descriptors. A perspective of this work would thus be to revisit the bonding of the diatomic molecules of presumably high bond multiplicities, in particular to check whether W_2 indeed represents a maximum of "covalency" after the introduction of the SOC, which was neglected in the seminal work of Roos *et al.* on EBOs [10].

Acknowledgments

This work has been supported in part by grants from the French National Agency for Research called "Investissements d'Avenir" (ANR-11-EQPX-0004, ANR-11-LABX-0018). It was carried out using HPC resources from CCIPL ("Centre de Calcul Intensif des Pays de la Loire"). P.A.B.H. and A.B. would like to acknowledge the Center for Information Technology of the University of Groningen for their support and for providing access to the

Peregrine high performance computing cluster.

---

[1] K. G. Dyall and K. Faegri Jr, Introduction to relativistic quantum chemistry (Oxford University Press, New York, 2007).

[2] L. Gagliardi and B. O. Roos, Nature **433**, 848 (2005).

[3] A. P. Sattelberger and M. J. A. Johnson, Science **337**, 652 (2012).

[4] X. Li, J. Comput. Chem. **35**, 923 (2014).

[5] L. Visscher and K. G. Dyall, J. Chem. Phys. **104**, 9040 (1996).

[6] C.-H. Hu, A. M. Asaduzzaman, and G. Schreckenbach, J. Phys. Chem. C **114**, 15165 (2010).

[7] J. Pilmé, E. Renault, T. Ayed, G. Montavon, and N. Galland, J. Chem. Theory Comput. **8**, 2985 (2012).

[8] R. Maurice, F. Réal, A. S. P. Gomes, V. Vallet, G. Montavon, and N. Galland, J. Chem. Phys. **142**, 094305 (2015).

[9] C. G. Pech, P. A. B. Haase, N. Galland, A. Borschevsky, and R. Maurice, Phys. Rev. A **100**, 032518 (2019).

[10] B. O. Roos, A. C. Borin, and L. Gagliardi, Angew. Chem. Int. Ed. **46**, 1469 (2007).

[11] T. Zeng, D. G. Fedorov, M. W. Schmidt, and M. Klobukowski, J. Chem. Theory Comput. **7**, 2864 (2011).

[12] F. Gendron, B. Le Guennic, and J. Autschbach, Inorg. Chem. **53**, 13174 (2014).

[13] D.-C. Sergentu, T. J. Duignan, and J. Autschbach, J. Phys. Chem. Lett. **9**, 5583 (2018).

[14] X. Zhang, W. Li, L. Feng, X. Chen, A. Hansen, S. Grimme, S. Fortier, D.-C. Sergentu, J. Duignan, Thomas, J. Autschbach, et al., Nat. Commun. **9**, 2753 (2018).

[15] S. Knecht, H. J. A. Jensen, and T. Saue, Nat. Chem. **11**, 40 (2019).

[16] R. F. W. Bader, Chem. Rev. **91**, 893 (1991).

[17] A. D. Becke and K. E. Edgecombe, J. Chem. Phys. **92**, 5397 (1990).

[18] B. Silvi and A. Savin, Nature **371**, 683 (1994).

[19] G. Eickerling, R. Mastalerz, V. Herz, W. Scherer, H.-J. Himmel, and M. Reiher, J. Chem. Theory Comput. **3**, 2182 (2007).

[20] E. Matito, P. Salvador, and J. Styszyński, Phys. Chem. Chem. Phys. **15**, 20080 (2013).

[21] J. Pilmé, E. Renault, F. Bassal, M. Amaouch, G. Montavon, and N. Galland, J. Chem. Theory

Comput. **10**, 4830 (2014).

[22] M. Amaouch, G. Montavon, N. Galland, and J. Pilmé, Mol. Phys. **114**, 1326 (2016).

[23] J. I. Rodríguez, E. A. Uribe, M. I. Baltazar-Méndez, J. Autschbach, F. Castillo-Alvarado, and I. Gutiérrez-González, Chem. Phys. Lett. **660**, 287 (2016).

[24] M. Amaouch, D.-C. Sergentu, D. Steinmetz, R. Maurice, N. Galland, and J. Pilmé, J. Comput. Chem. **38**, 2753 (2017).

[25] J. Graton, S. Rahali, J.-Y. Le Questel, G. Montavon, J. Pilmé, and N. Galland, Phys. Chem. Chem. Phys. **20**, 29616 (2018).

[26] M. De Santis, S. Rampino, H. M. Quiney, L. Belpassi, and L. Storchi, J. Chem. Theory Comput. **14**, 1286 (2018).

[27] J. S. M. Anderson, J. I. Rodríguez, P. W. Ayers, D. E. Trujillo-González, A. W. Götz, J. Autschbach, F. L. Castillo-Alvarado, and K. Yamashita, Chem. Eur. J. **25**, 2538 (2019).

[28] S. Sarr, J. Graton, G. Montavon, J. Pilmé, and N. Galland, ChemPhysChem **21**, 240 (2020).

[29] J. Karwowski and M. Stanke, Phys. Rev. A **71**, 024501 (2005).

[30] E. Engel and R. M. Dreizler, Density functional theory: An advanced course (Springer-Verlag, Berlin Heidelberg, 2011).

[31] L. Hedin and A. Johansson, J. Phys. B **2**, 1336 (1969).

[32] J. Champion, M. Seydou, A. Sabatié-Gogova, E. Renault, G. Montavon, and N. Galland, Phys. Chem. Chem. Phys. **13**, 14984 (2011).

[33] N. Guo, D.-C. Sergentu, D. Teze, J. Champion, G. Montavon, N. Galland, and R. Maurice, Angew. Chem. Int. Ed. **55**, 15369 (2016).

[34] N. Guo, R. Maurice, D. Teze, J. Graton, J. Champion, G. Montavon, and N. Galland, Nat. Chem. **10**, 428 (2018).

[35] L. Liu, N. Guo, J. Champion, J. Graton, G. Montavon, N. Galland, and R. Maurice, Chem. Eur. J. **26**, 3713 (2020).

[36] D.-C. Sergentu, M. Amaouch, J. Pilmé, N. Galland, and R. Maurice, J. Chem. Phys. **143**, 114306 (2015).

[37] D.-C. Sergentu, F. Réal, G. Montavon, N. Galland, and R. Maurice, Phys. Chem. Chem. Phys. **18**, 32703 (2016).

[38] C. Chang, M. Pelissier, and P. Durand, Phys. Scripta **34**, 394 (1986).

[39] J.-L. Heully, I. Lindgren, E. Lindroth, S. Lundqvist, and A.-M. Martensson-Pendrill, J. Phys.

B **19**, 2799 (1986).

[40] E. van Lenthe, E. J. Baerends, and J. G. Snijders, J. Chem. Phys. **99**, 4597 (1993).

[41] M. Douglas and N. M. Kroll, Ann. Phys. **82**, 89 (1974).

[42] B. A. Hess, Phys. Rev. A **33**, 3742 (1986).

[43] G. Jansen and B. A. Hess, Phys. Rev. A **39**, 6016 (1989).

[44] M. Barysz and A. J. Sadlej, J. Chem. Phys. **116**, 2696 (2002).

[45] M. Iliaš and T. Saue, J. Chem. Phys. **126**, 064102 (2007).

[46] M. Dolg and X. Cao, Chem. Rev. **112**, 403 (2012).

[47] B. O. Roos, P. Linse, P. E. M. Siegbahn, and M. R. A. Blomberg, Chem. Phys. **66**, 197 (1982).

[48] K. Andersson, P.-A. Malmqvist, B. O. Roos, A. J. Sadlej, and K. Wolinski, J. Phys. Chem. **94**, 5483 (1990).

[49] K. Andersson, P. Malmqvist, and B. O. Roos, J. Chem. Phys. **96**, 1218 (1992).

[50] K. G. Dyall, J. Chem. Phys. **102**, 4909 (1995).

[51] C. Angeli, R. Cimiraglia, S. Evangelisti, T. Leininger, and J.-P. Malrieu, J. Chem. Phys. **114**, 10252 (2001).

[52] C. Angeli, R. Cimiraglia, and J.-P. Malrieu, Chem. Phys. Lett. **350**, 297 (2001).

[53] C. Angeli, R. Cimiraglia, and J.-P. Malrieu, J. Chem. Phys. **117**, 9138 (2002).

[54] F. Gendron, D. Páez-Hernández, F.-P. Notter, B. Pritchard, H. Bolvin, and J. Autschbach, Chem. Eur. J. **20**, 7994 (2014).

[55] P.-O. Löwdin and H. Shull, Phys. Rev. **101**, 1730 (1956).

[56] E. R. Davidson, Rev. Mod. Phys. **44**, 451 (1972).

[57] A. Savin, O. Jepsen, J. Flad, O. K. Andersen, H. Preuss, and H. G. von Schnering, Angew. Chem. Int. Ed. **31**, 187 (1992).

[58] E. Matito, B. Silvi, M. Duran, and M. Solà, J. Chem. Phys. **125**, 024301 (2006).

[59] F. Feixas, E. Matito, M. Duran, M. Solà, and B. Silvi, J. Chem. Theory Comput. **6**, 2736 (2010).

[60] A. Savin, B. Silvi, and F. Colonna, Can. J. Chem. **74**, 1088 (1996).

[61] M. Kohout, K. Pernal, F. R. Wagner, and Y. Grin, Theor. Chem. Acc. **112**, 453 (2004).

[62] A. M. K. Müller, Phys. Lett. A **105**, 446 (1984).

[63] M. A. Buijse and E. J. Baerends, Mol. Phys. **100**, 401 (2002).

[64] R. F. W. Bader and M. E. Stephens, J. Am. Chem. Soc. **97**, 7391 (1975).

[65] X. Fradera, M. A. Austen, and R. F. W. Bader, J. Phys. Chem. A **103**, 304 (1999).

[66] Y.-G. Wang and N. H. Werstiuk, J. Comput. Chem. **24**, 379 (2003).

[67] J. Autschbach, Comments Inorg. Chem. **36**, 215 (2016).

[68] S. Noury, X. Krokidis, F. Fuster, and B. Silvi, Comput. Chem. **23**, 597 (1999).

[69] H.-J. Werner, P. J. Knowles, G. Knizia, F. R. Manby, M. Schütz, P. Celani, W. Györffy, D. Kats, T. Korona, R. Lindh, et al., Molpro, a package of ab initio programs, version 2015.1 (2015).

[70] I. N. Levine, Quantum Chemistry, Fifth Edition (Prentice-Hall, Upper Saddle River, 1999).

[71] T. Petersson and B. Hellsing, Eur. J. Phys. **31**, 37 (2009).

[72] L. Visscher, T. J. Lee, and K. G. Dyall, J. Chem. Phys. **105**, 8769 (1996).

[73] A. S. P. Gomes, F. Réal, N. Galland, C. Angeli, R. Cimiraglia, and V. Vallet, Phys. Chem. Chem. Phys. **16**, 9238 (2014).

[74] L. Visscher, H. J. Aa. Jensen, R. Bast, and T. Saue, with contributions from V. Bakken, K. G. Dyall, S. Dubillard, U. Ekström, E. Eliav, T. Enevoldsen, E. Faßhauer, T. Fleig, O. Fossgaard, A. S. P. Gomes, E. D. Hedegård, T. Helgaker, J. Henriksson, M. Iliaš, Ch. R. Jacob, S. Knecht, S. Komorovský, O. Kullie, J. K. Lærdahl, C. V. Larsen, Y. S. Lee, H. S. Nataraj, M. K. Nayak, P. Norman, G. Olejniczak, J. Olsen, J. M. H. Olsen, Y. C. Park, J. K. Pedersen, M. Pernpointner, R. di Remigio, K. Ruud, P. Sałek, B. Schimmelpfennig, A. Shee, J. Sikkema, A. J. Thorvaldsen, J. Thyssen, J. van Stralen, S. Villaume, O. Visser, T. Winther, and S. Yamamoto. DIRAC, a relativistic ab initio electronic structure program, release DIRAC15 (2015), see: http://www.diracprogram.org.

[75] K. G. Dyall, Theor. Chem. Acc. **115**, 441 (2006).

[76] K. G. Dyall, Theor. Chem. Acc. **135**, 128 (2016).

[77] L. Visscher and K. G. Dyall, At. Data Nucl. Data Tables **67**, 207 (1997).

[78] K. A. Peterson, D. Figgen, E. Goll, H. Stoll, and M. Dolg, J. Chem. Phys. **119**, 11113 (2003).

[79] K. A. Peterson, B. C. Shepler, D. Figgen, and H. Stoll, J. Phys. Chem. A **110**, 13877 (2006).

[80] R. A. Kendall, T. H. Dunning, and R. J. Harrison, J. Chem. Phys. **96**, 6796 (1992).

[81] D. E. Woon and T. Dunning, J. Chem. Phys. **98**, 1358 (1993).

[82] C. Outeiral, M. A. Vincent, A. Martín Pendás, and P. L. A. Popelier, Chem. Sci. **9**, 5517 (2018).

[83] S. Shaik, D. Danovich, B. Silvi, D. L. Lauvergnat, and P. C. Hiberty, Chem. Eur. J. **11**, 6358

(2005).

[84] S. Shaik, D. Danovich, W. Wu, and P. C. Hiberty, Nat. Chem. **1**, 443 (2009).

[85] H. Zhang, D. Danovich, W. Wu, B. Braïda, P. C. Hiberty, and S. Shaik, J. Chem. Theory Comput. **10**, 2410 (2014).

[86] P. C. Hiberty, S. Humbel, D. Danovich, and S. Shaik, J. Am. Chem. Soc. **117**, 9003 (1995).

[87] K. R. Loos and A. C. Jones, J. Phys. Chem. **78**, 2306 (1974).

[88] B. Braïda and P. C. Hiberty, J. Phys. Chem. A **112**, 13045 (2008).

[89] B. Braïda and P. C. Hiberty, J. Am. Chem. Soc. **126**, 14890 (2004).

[90] T. Clark, J. S. Murray, and P. Politzer, ChemPhysChem **19**, 3044 (2018).

[91] R. Maurice. On the role of relativistic effects on the structural, physical and chemical properties of molecules and materials, Habilitation thesis, University of Nantes (2018), see: https://tel.archives-ouvertes.fr/tel-02308305.

[92] A. D. Becke, The Journal of Chemical Physics **98**, 1372 (1993).

[93] P. J. Stephens, F. J. Devlin, C. F. Chabalowski, and M. J. Frisch, J. Phys. Chem. **98**, 11623 (1994).

[94] B. Silvi, Phys. Chem. Chem. Phys. **6**, 256 (2004).

[95] E. Matito and M. Solà, Coord. Chem. Rev. **253**, 647 (2009).

[96] T. Ayed, J. Pilmé, D. Tézé, F. Bassal, J. Barbet, M. Chérel, J. Champion, R. Maurice, G. Montavon, and N. Galland, Eur. J. Med. Chem. **116**, 156 (2016).

[97] N. Galland, G. Montavon, J.-Y. Le Questel, and J. Graton, New J. Chem. **42**, 10510 (2018).

[98] D. S. Wilbur, Nat. Chem. **5**, 246 (2013).

Table of contents:

Artwork:

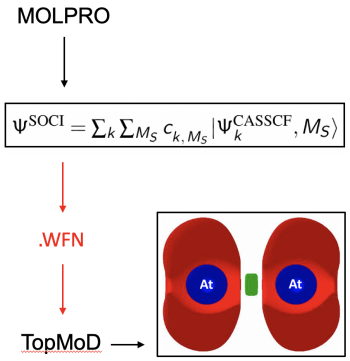

Synopsis:

We report a new methodology that allows to perform topological analyses (QTAIM and ELF) at the spin-orbit configuration interaction level. It is applied to unravel the chemical bonding in astatine ($Z = 85$) compounds, for which the spin-orbit coupling plays a significant role on the bonds. This methodology can be readily applied to the ground and excited states of any compound, with a reliability that is ensured up to the heavy elements.